Title	Stator-flux-oriented fault-tolerant control of flux-switching permanent-magnet motors
Author(s)	Zhao, W; Cheng, M; Chau, KT; Hua, W; Jia, H; Ji, J; Li, W
Citation	The IEEE International Magnetic Conference (INTERMAG2011), Taipei, Taiwan, 25-29 April 2011. In IEEE Transactions on Magnetics, 2011, v. 47 n. 10, p. 4191-4194
Issued Date	2011
URL	http://hdl.handle.net/10722/155669
Rights	©2011 IEEE. Personal use of this material is permitted. However, permission to reprint/republish this material for advertising or promotional purposes or for creating new collective works for resale or redistribution to servers or lists, or to reuse any copyrighted component of this work in other works must be obtained from the IEEE.

Stator-Flux-Oriented Fault-Tolerant Control of Flux-Switching Permanent-Magnet Motors

Wenxiang Zhao[1,2], Ming Cheng[1], K. T. Chau[1,3], Wei Hua[1], Hongyun Jia[1], Jinghua Ji[2], and Wenlong Li[3]

[1]School of Electrical Engineering, Southeast University, Nanjing 210096, China
[2]School of Electrical and Information Engineering, Jiangsu University, Zhenjiang 212013, China
[3]Department of Electrical and Electronic Engineering, The University of Hong Kong, Hong Kong

Flux-switching permanent-magnet (FSPM) motors are a newly developed brushless AC (BLAC) machine having magnets in the stator. This paper proposes and implements a stator-flux-oriented (SFO) control strategy for fault-tolerant operation of FSPM motors. The key is to set the q-axis component of armature current invariant before and after the fault. In the rotor reference frame, by building a SFO-dq equation of the FSPM motor, the fault-tolerant control strategy is deduced. The finite-element method and the field-circuit cosimulation method are employed to analyze the performance of the FSPM motor drive. Finally, a dSPACE-based FSPM motor drive platform is built for experimental verification. Both the steady-state and dynamic performances at normal and fault-tolerant operations are tested, confirming that the proposed fault-tolerant operation can keep the output torque invariant while offering good dynamic performance during fault.

***Index Terms*—Fault-tolerant control, flux switching, permanent-magnet motor, stator-flux oriented (SFO).**

I. Introduction

FAULT tolerance of motor drives is important for critical applications desiring continued operation following a fault such as electric vehicle applications [1]. In recent years, some fault-tolerant machines, namely the switched reluctance (SR) machine [2] and the conventional permanent-magnet (PM) brushless machine having magnets in the rotor (the rotor-PM machine) [3], have been developed. However, the SR machine still suffers from relatively low power density, while the rotor-PM machine is still hindered by weak mechanical structure [4]. Recently, a new class of brushless machines with PMs located in the stator, namely the stator-PM machine, has been proposed, which offers high power density and good mechanical integrity [5]–[7]. It has been identified that the doubly-salient PM (DSPM) motor can inherently offer fault tolerance [8], [9]. On the other hand, recent research has verified that the power density of a flux-switching PM (FSPM) motor is significantly higher than that of a DSPM motor [10]. Hence, how to improve the fault-tolerance capability of FSPM motors has attracted more and more attention.

In recent years, some fault-tolerant FSPM motors have been developed. By incorporating the modular structure, alternate poles, and redundant windings into the existing motor design [11]–[13], the fault-tolerance capability can be achieved. However, differing from using design approaches, the use of control strategies takes the advantages of flexible and directly applicable to the existing FSPM motors.

This paper presents a stator-flux-oriented (SFO) fault-tolerant control strategy for FSPM motors, which can keep the output torque invariant while offering good dynamic performance during fault. The remedial operation mode will be investigated and then verified by both simulation and experimentation. It should be noted that the SFO control for fault-tolerant operation of FSPM motors is absent in literature.

Manuscript received February 21, 2011; accepted May 11, 2011. Date of current version September 23, 2011. Corresponding author: W. Zhao (e-mail: zwx@ujs.edu.cn).

Color versions of one or more of the figures in this paper are available online at http://ieeexplore.ieee.org.

Digital Object Identifier 10.1109/TMAG.2011.2157106

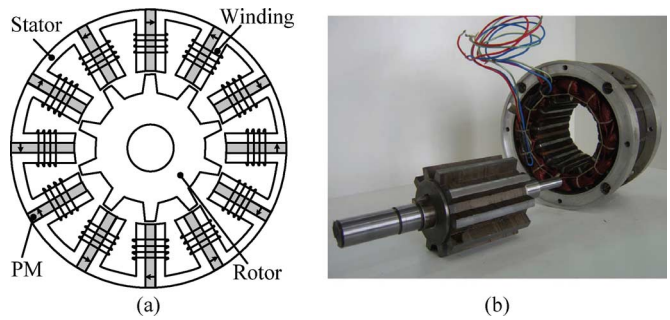

Fig. 1. Three-phase 12/10-pole FSPM motor. (a) Schematic. (b) Prototype.

II. Analysis and Control

A. FSPM Motor

A three-phase 12/10-pole FSPM motor is shown in Fig. 1, in which the rotor has only solid-iron salient poles while the stator incorporates both PMs and armature windings. Since there are no PMs, brushes, or windings in the rotor, the FSPM motor offers the advantages of simple rotor configuration and mechanical robustness. By adopting high-energy PM as excitation, the FSPM motor retains the merits of the rotor-PM motor, such as high efficiency and power density. Also, since all PMs are located in the stator, the problems of cooling difficulty and thermal instability in the rotor-PM motor can be eliminated.

Moreover, the finite-element method (FEM) is employed to analyze the characteristics of the FSPM motor. Fig. 2 compares the flux vectors due to the PMs and the armature winding current. It can be seen that their flux paths are in parallel, which differs from the series nature of those flux paths in other PM motors. Thus, the possibility of demagnetization of PMs by armature reaction flux under the short-circuit fault is eliminated, providing the capability of fault tolerance.

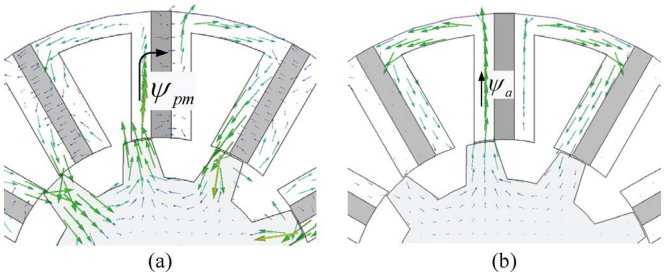

Fig. 2. Comparison of flux vectors. (a) PMs only. (b) Armature current only.

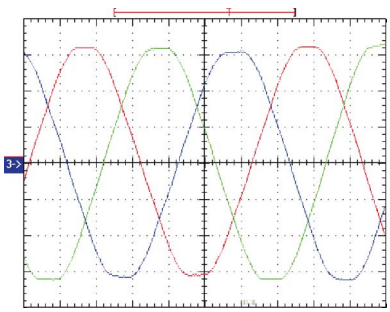

Fig. 3. Measured three-phase no-load EMF waveforms (1 ms/div, 50 V/div).

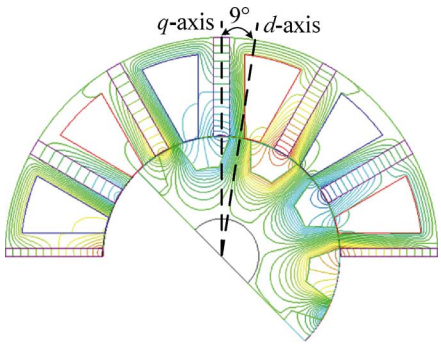

Fig. 4. No-load field distribution and axis definition.

B. Stator-Flux Orientation

Fig. 3 shows the measured no-load EMF waveforms of the FSPM motor, where their shapes are approximately sinusoidal. Thus, the FSPM motor is particularly suitable for brushless AC (BLAC) operation and the vector control can be employed. However, since the FSPM motor does not generate rotational magnetomotive force (MMF), the traditional rotor-flux-oriented control strategy cannot be applied to the FSPM motor directly.

In order to enable vector control in this FSPM motor, a SFO-dq equation of the motor in the rotor reference frame is developed. Fig. 4 shows the FEM-based no-load magnetic field distribution, in which the relative positions between the d- and q-axes, and the stator teeth and rotor poles are depicted. It can be found that the rotor position of the maximum PM flux linkage is defined as the d-axis, while the q-axis advances the d-axis by 90° in electrical degrees (equivalent to 9° in mechanical degrees). The development of the dq-axes is crucial for the development of this SFO fault-tolerant control strategy.

C. Fault-Tolerant Control Strategy

It has been known that the q- and d-axis components of armature currents correspond to the production of torque and flux, respectively. When the d-axis component of armature current is maintained, the stator-PM flux-linkage will be constant. Thus, by setting the q-axis component of armature current invariant before and after the fault, the electromagnetic torque of the FSPM motor can be maintained.

Based on the proposed SFO, the armature currents of the FSPM motor during normal operation can be expressed as

$$\begin{cases} i_a = i_d \cos\theta - i_q \sin\theta \\ i_b = i_d \cos(\theta - 2\pi/3) - i_q \sin(\theta - 2\pi/3) \\ i_c = i_d \cos(\theta + 2\pi/3) - i_q \sin(\theta + 2\pi/3) \end{cases} \tag{1}$$

where θ is the rotor angle, i_a, i_b, and i_c are the phase currents, and i_d and i_q are the transformed currents in the synchronous reference frame. The α-β-0 to a-b-c transformation can be written as

$$\begin{bmatrix} i_a \\ i_b \\ i_c \end{bmatrix} = \begin{bmatrix} 1 & 0 & 1 \\ -\frac{1}{2} & \frac{\sqrt{3}}{2} & 1 \\ -\frac{1}{2} & -\frac{\sqrt{3}}{2} & 1 \end{bmatrix} \begin{bmatrix} i_\alpha \\ i_\beta \\ i_0 \end{bmatrix} \tag{2}$$

where i_α and i_β are the transformed currents in the fixed stator reference frame, and i_0 is the zero-sequence current.

When the phase-A winding is open circuited, the phase-A current vanishes so that the motor is fed by two healthy phases. The zero-sequence component of armature current can be obtained as

$$i_0 = -i_\alpha. \tag{3}$$

Then, by substituting (3) into (2), it deduces

$$\begin{cases} i'_a = 0 \\ i'_b = -\frac{3}{2} i_\alpha + \frac{\sqrt{3}}{2} i_\beta \\ i'_c = -\frac{3}{2} i_\alpha - \frac{\sqrt{3}}{2} i_\beta. \end{cases} \tag{4}$$

The d-q to α-β transformation can be written as

$$\begin{bmatrix} i_\alpha \\ i_\beta \end{bmatrix} = \begin{bmatrix} \cos\theta & -\sin\theta \\ \sin\theta & \cos\theta \end{bmatrix} \begin{bmatrix} i_d \\ i_q \end{bmatrix}. \tag{5}$$

Then, by substituting (5) into (4), the fault-tolerant control strategy can be deduced as

$$\begin{cases} i'_a = 0 \\ i'_b = \sqrt{3}[i_d \cos(\theta - 5\pi/6) - i_q \sin(\theta - 5\pi/6)] \\ i'_c = \sqrt{3}[i_d \cos(\theta + 5\pi/6) - i_q \sin(\theta + 5\pi/6)]. \end{cases} \tag{6}$$

Fig. 5 shows the control block diagram of the FSPM motor drive, in which the SFO fault-tolerant control is incorporated. By employing a proportional–integral (PI) regulator, the difference between the reference speed and the actual speed determines the reference electromagnetic torque, which is directly proportional to the q-axis component of armature current. The hysteresis PWM controller is employed to drive the inverter. During the fault-tolerant operation, the FSPM motor operates in the two-phase mode. The q-axis component of armature current

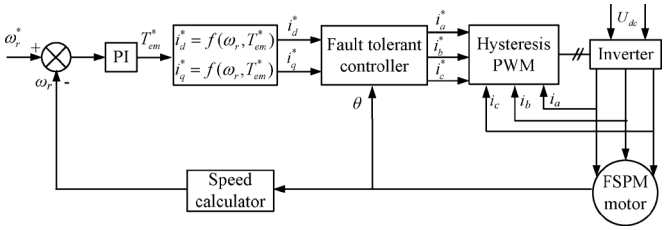

Fig. 5. Control block diagram of fault-tolerant FSPM motor drive.

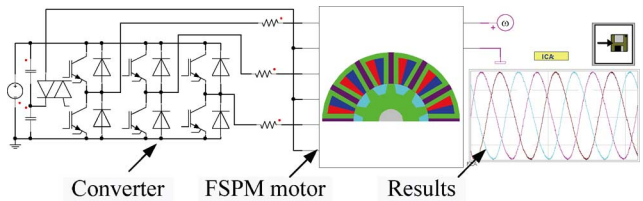

Fig. 6. Cosimulation model of FSPM motor drive.

can be set invariant before and after the fault, thus maintaining the average torque during the fault-tolerant operation.

III. Results and Verification

A. Simulation

To evaluate the proposed remedial control strategy, a transient coupling field-circuit cosimulation model of the FSPM motor drive is developed as shown in Fig. 6. The cosimulation method simultaneously employs both the magnetic field solver and the electric circuit solver, thus providing an accurate system level simulation [8].

For the purpose of quantitative evaluation of torque performance of the FSPM motor drive under normal and fault-tolerant operations, a torque ripple factor is defined as

$$K_T = (T_{\max} - T_{\min})/T_{\text{av}} \times 100\% \tag{11}$$

where $T_{\max}, T_{\min}$, and T_{av} are the maximum, minimum, and average values of the output torque, respectively.

During the normal and fault-tolerant operations of the FSPM motor drive, the cosimulated torque and current waveforms are obtained as shown in Fig. 7. It can be seen that under the normal operation, the corresponding T_{av} and K_T of the motor drive are 6.7 Nm and 58.9%, respectively. It should be noted that the torque ripple is mainly caused by the cogging torque of the FSPM motor [7]. Quantitatively, the T_{av} and K_T of the FSPM motor drive under fault-tolerant operation are 6.6 Nm and 62.7%, respectively. It can be concluded from these results that the torque performances under the normal and fault-tolerant operation are practically unchanged. A slight discrepancy is mainly due to the nonideal sinusoidal no-load EMFs of the FSPM motor.

B. Experimentation

A prototype of the FSPM motor drive is built for experimental verification of the proposed fault-tolerant control. The test bench consists of the FSPM motor, a DC dynamometer to serve as variable load, a dynamic torque transducer to measure

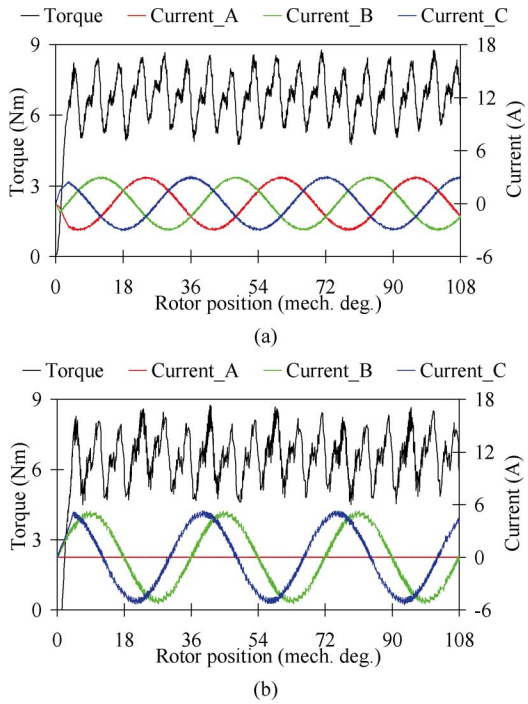

Fig. 7. Simulated torque and current waveforms. (a). Normal operation. (b) Fault-tolerant operation.

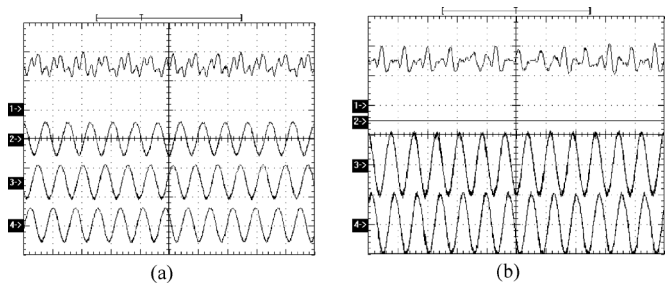

Fig. 8. Measured steady-state torque (trace 1) and current (traces 2–4) waveforms (25 ms/div, 4 Nm/div, 4.8 A/div). (a) Normal operation. (b) Fault-tolerant operation.

the torque waveform, and a dSPACE-based digital controller to implement the control scheme. In addition, an optical position encoder and three Hall-effect current sensors are used for measurement.

First, the proposed remedial operation of the FSPM motor is assessed during steady-state operation. Fig. 8 compares the steady-state torque and current waveforms under normal and faulty conditions. It can be seen that the measured waveforms agree with the simulated ones as shown in Fig. 7, verifying that the proposed remedial operation can maintain the same torque during the loss of one phase.

Then, the proposed fault-tolerant control strategy is evaluated during dynamic operation. Fig. 9(a) shows the healthy phase current responses before and after fault-tolerant operation. It can be observed that the motor drive can online switch to the fault-tolerant mode.

Furthermore, the self-starting capability under the open-circuit fault is particularly assessed, which is essential for those ap-

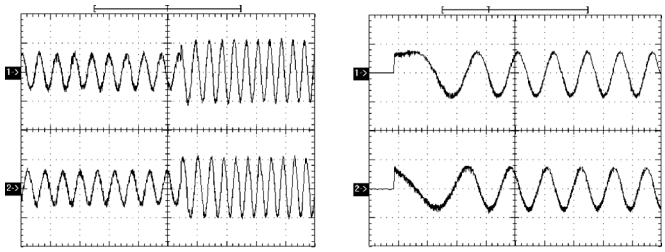

Fig. 9. Measured dynamic current responses of healthy phases. (a) Before and after fault (50 ms/div, 4.8 A/div). (b) Startup (25 ms/div, 12 A/div).

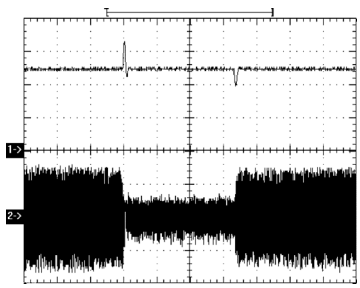

Fig. 10. Measured speed (trace 1) and current (trace 2) responses under sudden load changes (5 s/div, 200 rpm/div, 2.4 A/div).

plications such as electric vehicles desiring frequent start–stop. Fig. 9(b) shows the startup current responses under fault-tolerant operation, confirming that the motor drive can successfully perform self-starting during the loss of one phase.

Finally, the dynamic load test of the developed motor drive at fault-tolerant operation is performed. Fig. 10 depicts the dynamic responses of speed and current under sudden changes of load torque (from 7.2 to 2.5 Nm and then back to 7.2 Nm) when the motor operates in the fault-tolerant mode. It can be found that the transient changes in speed are quite small, while the speed regulation is very good.

IV. Conclusion

In this paper, the SFO control strategy has been newly applied for fault-tolerant operation of FSPM motors. By setting the q-axis component of armature current invariant before and after the fault, the output torque can be maintained constant while offering good dynamic performance during fault. Both the field-circuit cosimulation and experimental results confirm the validity of the proposed fault-tolerant control strategy for FSPM motors. This control strategy can readily be extended to other types of stator-PM motors that can operate at the BLAC mode.

Acknowledgment

This work was supported in part by the National Natural Science Foundation of China (Projects 60974060, 50907031, and 51007031), by the Aeronautical Science Foundation of China (Project 20100769004), and by the Professional Research Foundation for Advanced Talents of Jiangsu University, China (Project 10JDG089).

References

[1] K. T. Chau and C. C. Chan, "Emerging energy-efficient technologies for hybrid electric vehicles," *Proc. IEEE*, vol. 95, no. 4, pp. 821–835, Apr. 2007.

[2] M. Bouji, A. A. Arkadan, and T. Ericsen, "Fuzzy inference system for the characterization of SRM drives under normal and fault conditions," *IEEE Trans. Magn.*, vol. 37, no. 5, pp. 3745–3748, Sep. 2001.

[3] J. Wang, K. Atallah, and D. Howe, "Optimal torque control of fault-tolerant permanent magnet brushless machines," *IEEE Trans. Magn.*, vol. 39, no. 5, pp. 2962–2964, Sep. 2003.

[4] Z. Q. Zhu and D. Howe, "Electrical machines and drives for electric, hybrid, and fuel cell vehicles," *Proc. IEEE*, vol. 95, no. 4, pp. 746–765, Apr. 2007.

[5] C. Liu, K. T. Chau, J. Jiang, and S. Niu, "Comparison of stator-permanent-magnet brushless machines," *IEEE Trans. Magn.*, vol. 44, no. 11, pp. 4405–4408, Nov. 2008.

[6] Y. Gong, K. T. Chau, J. Z. Jiang, C. Yu, and W. Li, "Design of doubly salient permanent magnet motors with minimum torque ripple," *IEEE Trans. Magn.*, vol. 45, no. 10, pp. 4704–4707, Oct. 2009.

[7] Z. Q. Zhu and J. T. Chen, "Advanced flux-switching permanent magnet brushless machines," *IEEE Trans. Magn.*, vol. 46, no. 6, pp. 1447–1453, Jun. 2010.

[8] W. Zhao, K. T. Chau, M. Cheng, J. Ji, and X. Zhu, "Remedial brushless AC operation of fault-tolerant doubly-salient permanent-magnet motor drives," *IEEE Trans. Ind. Electron.*, vol. 57, no. 6, pp. 2134–2141, Jun. 2010.

[9] C. Liu, K. T. Chau, and W. Li, "Comparison of fault-tolerant operations for permanent-magnet hybrid brushless motor drive," *IEEE Trans. Magn.*, vol. 46, no. 6, pp. 1378–1381, Jun. 2010.

[10] J. Zhang, M. Cheng, Z. Chen, and W. Hua, "Comparison of stator-mounted permanent-magnet machines based on a general power equation," *IEEE Trans. Energy Conv.*, vol. 24, no. 4, pp. 826–834, Dec. 2009.

[11] M. Jin, C. Wang, J. Shen, and B. Xia, "A modular permanent-magnet flux-switching linear machine with fault-tolerant capability," *IEEE Trans. Magn.*, vol. 45, no. 8, pp. 3179–3186, Aug. 2009.

[12] R. L. Owen, Z. Q. Zhu, A. S. Thomas, G. W. Jewell, and D. Howe, "Alternate poles wound flux-switching permanent-magnet brushless AC machines," *IEEE Trans. Ind. Appl.*, vol. 46, no. 2, pp. 790–797, Mar./Apr. 2010.

[13] W. Zhao, M. Cheng, W. Hua, H. Jia, and R. Cao, "Back-EMF harmonic analysis and fault-tolerant control of flux-switching permanent-magnet machine with redundancy," *IEEE Trans. Ind. Electron.*, vol. 58, no. 5, pp. 1926–1936, May 2011.